People's Democratic Republic of Algeria

Ministry of Higher Education and Scientific Research

University M'Hamed BOUGARA- Boumerdes

Institute of Electrical and Electronic

Engineering

Department of Electronics

Project Report Presented in Partial Fulfilment of

the Requirements of the Degree of

'MASTER'

In **Telecommunication**

Option: **Telecommunications**

Title:

Design of a Two-port MIMO Antenna with Low-Mutual Coupling Based on a Pentagonal-Fractal Ring Element

Presented By:

- **MOKRANI Mohamed Amine**

Supervisor:

Dr. K DJAFRI

June 2024

Abstract

In this work, a two-element multiple-input–multiple-output (MIMO) 3.5GHz antenna covering the 3.5 WiMAX commercially useful application is proposed and analyzed. The antenna element is based on first-order pentagonal fractal ring monopole antenna fed by a Y-shaped transmission line. To achieve a compact size, the sides on the pentagonal ring are loaded with a triangular shaped branches oriented towards the antenna center to obtain the fractal ring radiating element. The resulted antenna element , overall dimensions of 15x19mm2 , is fabricated and its reflection coefficient is measured for experimental validation. The resulted antenna element is then used to design a two-port MIMO antenna. The MIMO antenna consists of two identical antenna elements arranged orthogonally in polarization diversity configuration. By loading the antenna with a rectangular stub, the mutual coupling between the antenna elements is significantly reduced. The stub is printed diagonally in the back side of the substrate. The resulted MIMO antenna has an overall size of $31.35x31.35mm2$ with better isolation less then -19 dB. The simulated maximum realized gain and maximum radiation efficiency are $1.76dBi$ and 66.33% respectively. Moreover, the performance of the proposed MIMO antenna in terms of isolation, realized gain, radiation efficiency and radiation patterns are studied.

Acknowledgement

We are primarily grateful to Allah, the Most Gracious and Merciful, for enabling us to finish this menial task. Our faith in him got us through the most trying periods when it looked like there was no way out.

It gives me great pleasure to convey my sincere gratitude and admiration to everyone who has given me academic assistance and mental fortitude. Dr. K.DJAFRI, who oversaw my final year project and saw it through to the very finish. Her unwavering patience, encouragement, and direction helped us to successfully complete the job.

Not to forget my precious family members who accompanied me throughout the whole journey.

Dedication

This dedication is for the greatest treasure I have ever had, and always will have, is my family.To my parents, Father Toumi and Mother Habiba, for making me the person I am today and supporting me with all the possible ways.

To my dear sisters, who have never left my side and have helped me out in every way possible. Wishing them a happy and succeful life

To my friends A.Bedr-eddine Z.Amor A.Heythem H.Hadj R.Aboubaker M.Houcine M.Ahmed A.Hamada B.Yuba O.Anis B.Raouf A.Abderezak Mohamed Walid Zin-eddine wishing them all the best in their life

Contents

List of Figures

List of Tables

List of Abbreviations

MPA	Microstrip Patch Antenna
PCB	Printed Circuit Board
PIFA	Planar Inverted Frequency Antenna
DGS	Defected Ground Structure
BPSK	Binary Phase Shift Keying
2D	Two-Dimensional
3D	Three-Dimensional
CST	Computer Simulation Technology
FR-4	Flame Resistant 4
MIMO	Multiple Input Multiple Output
SNR	Signal to Noise Ratio
WiMAX	Worldwide Interoperability for Microwave Access
S11	Reflection Coefficient
S21	The Isolation
RFID	Radio Frequency Identification
dB	decibel scale
dBi	decibels relative to isotropic
PRPA	Pentagonal Ring Patch Antenna
FPRA	Fractal Pentagonal Ring Antenna
MPRA	Modified Pentagonal Ring Patch Antenna
VNA	Vector Network Analyzer

List of Symbols

Γ	Reflection coefficient.
Z_{in}	the input impedance of the antenna.
Z_0	the characteristic impedance of the transmission (feed) line.
D	directivity.
Dmax	maximum directivity.
U	radiation intensity.
U_0	average radiation intensity.
P_{in}	total input (accepted)power.
P_{rad}	radiated power.
G	gain.
ϕ	the elevation angle.
θ	the azimuth angle.
h	substrate thickness.
ϵ_r	relative permittivity.

General Introduction

An antenna is defined by Webster's Dictionary as "a usually metallic device (as a rod or wire) for radiating or receiving radio waves." The IEEE Standard Definitions of Terms for Antennas defines the antenna or aerial as "a means for radiating or receiving radio waves." In other words the antenna is the transitional structure between free-space and a guiding device. The guiding device or transmission line may take the form of a coaxial line or a hollow pipe (waveguide), and it is used to transport electromagnetic energy from the transmitting source to the antenna, or from the antenna to the receiver. In the former case, we have a transmitting antenna and in the latter a receiving antenna[1]. Multiple input multiple output (MIMO) antenna technology is evolved as an essential part in fourth and fifth generations of wireless applications due to its advantages over a single radiating element on low cost printed circuit boards (PCBs). Involvement of MIMO leads to the high data rate, low power consumption, spectrum saving, large capacity, and better quality of services (QOS) in non-line-of-sight (NLOS) communication. MIMO antennas have a lot of capabilities and qualities but highly affected by the mutual coupling of closely packed radiators, which is one of the challenges in MIMO antenna designs[2].

In this work, two element MIMO antenna of fractal shaped pentagonal ring antenna is presented and studied. The pentagonal fractal ring radiating element is designed to resonant at 3.5 GHz. In addition, a partial rectangular ground plane is used to increase the operating frequency bandwidth and reduce the antenna dimensions. After that, two elements MIMO antenna is derived by placing the its elements on x and y axis at the corner of the substrate. The inter-port isolation is improved by loading the antenna ground plane by a rectangular stub placed diagonally. The single antenna element and the MIMO configuration are designed and analyzed using a full wave simulator CST and printed on the FR-4 substrate.

The report includes three main chapters and it is organized as follows:

Chapter 1 presents an overview on Microstrip Patch Antenna (MPA) including a general description, fundamental operating principles, feeding methodology, advantages and disadvantages. In addition, the chapter introduces MIMO antenna systems together with basic parameters, types, applications and isolation techniques.

Chapter 2 gives the different steps of designing the pentagonal fractal ring antenna shaped operating in the frequency band extending from 3.20 GHz to 3.85 GHz centred at 3.5 GHz. Three intermediate structures are considered and theirs reflection coefficients over the considered range of frequency are simulated and analyzed.

Chapter 3 focuses on the analysis of the proposed MIMO antenna. The high isolation between the antenna elements is achieved by orthogonal placing of the antenna elements and by inserting a rectangular stub in the antenna ground plane .To gain a better knowledge of the working and isolation mechanisms, a thorough parametric study is also conducted for the suggested structure.

A conclusion is presented at the end of the report.

Chapter 1

Theory of Microstrip Antennas and MIMO Technology

1.1 Introductionto Microstrip Patch Antennas

Antenna is a device that is used to transmit and receive the information in the form of electromagnetic waves only. Antenna is generally classified according to the frequencies, low-frequency, medium-frequency, and high-frequency antenna[2]. In its simplest form, a MPA consists of a metallic patch placed on a dielectric material and supported by a ground plane. It can be easily fabricated on printed circuit board.1.1 The mostly used configuration is shown the Figure 1.1.

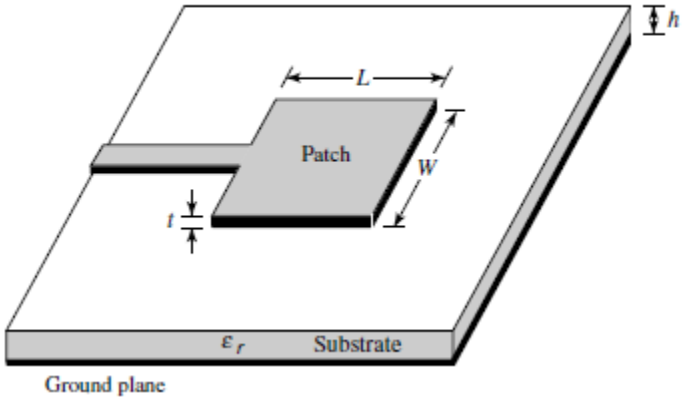

Figure 1.1: Microstrip Patch Antenna[1]

Microstrip antennas were first developed in the 1950's. However, this concept had to wait for about 20 years to be realized after the development of the printed circuit board (PCB) technology in the 1970's. Since then, microstrip antennas are the most common types of antennas with wide range of applications due to their apparent advantage of light weight, low profile, low cost, planar configuration, ease of conformal, superior potability, suitable for array with the simple way of fabrication and integration with microwave monolithic integrate circuits (MMICs). They have been widely engaged for the civilian and military applications such as radio-frequency identification (RFID), television, multiple input multiple output (MIMO) systems, WLAN, and WiMax [4].

In view of this, High-frequency MSAs are the antennas in which dielectric substrates are between the radiating patch and ground plane and are shown in Figure 1.2 along with its equivalent circuit diagram. Patch antenna at high frequency is represented as a parallel combination resistance R1, capacitance C1, and inductance L1. The value and equations of

C1, R1, and L1 vary depending on the shape and size of antennas [2]. Patch antennas can

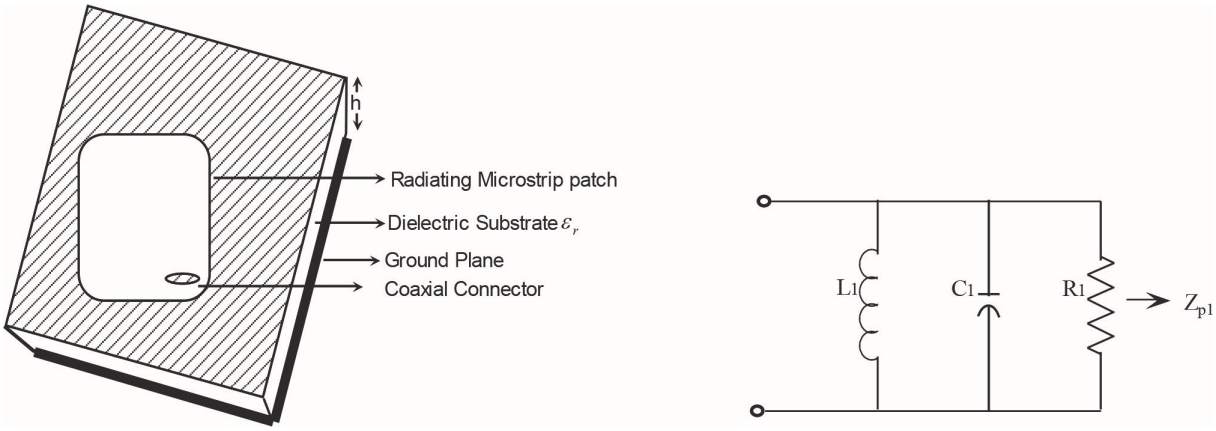

Figure 1.2: Configuration of microstrip antenna and its equivalent circuit diagram[2]

be of any shape and size. Figure 1.3 shows different types of existing geometry of antennas such as square, rectangular, circle, elliptical, triangular, sectorial, angular ring, semicircular, and square ring. First microstrip patch antenna was reported by Deschamp [5] in 1953. High-frequency microstrip patch antennas generally are divided according to the frequency bands, i.e., dual-band, multiband, broadband, and ultra-wideband (UWB).

1.2 Multiband MSAs

Dual-band and multiband microstrip patch antenna can be realized with different techniques such as stacking, coplanar structures (parasitic patches), slots, notches, shorting pin, shorting wall and active devices, etc. Using these techniques several research papers were published by various researchers, and the first dual-band radiator was reported in 1984, using shorting pins in rectangular patches by Wang and Lo [6]. In this section, literature survey of dual-band and multiband is presented on the basis of techniques used to achieve dual or multiband.

1.2.1 Slot loaded MSAs

Slot loaded MSAs can be achieved by etching rectangular or slot of any desired shape in the patch as shown in Figure 1.4 This antenna can be represented as a parallel combination of impedance due to patch (Zp1) and impedance due to slot (Zsh), and its equivalent is denoted

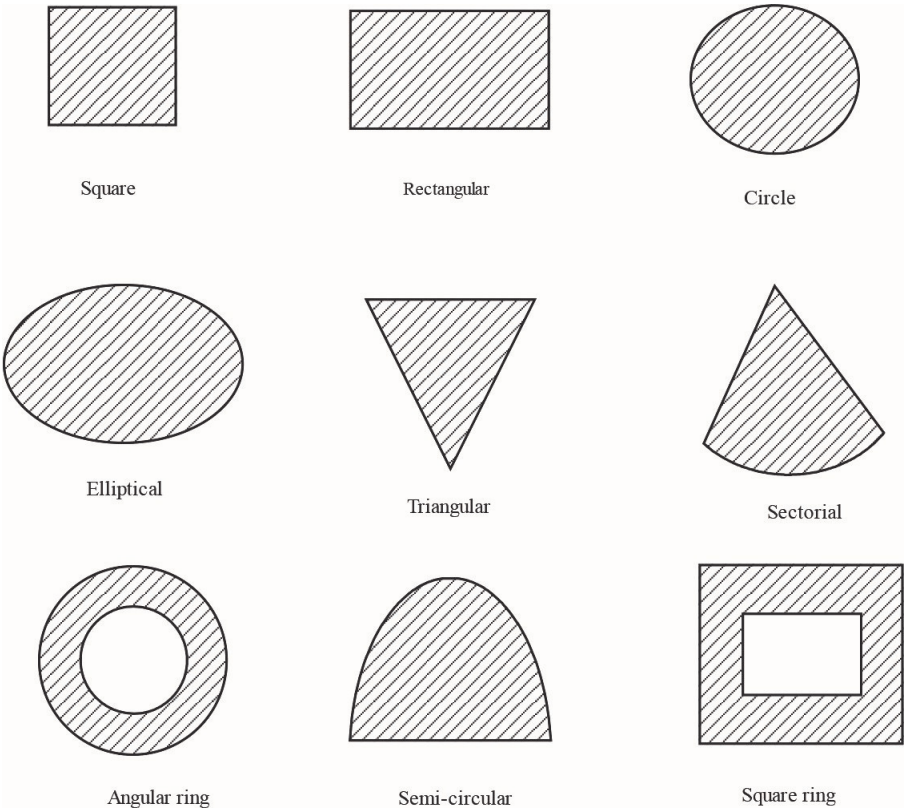

Figure 1.3: Different shapes of radiating patches [2]

as (Zps)[2], as given in Figure 3 and calculated as,

$$\frac{1}{Zps} = \frac{1}{Zp1} + \frac{1}{Zsh} \tag{1.1}$$

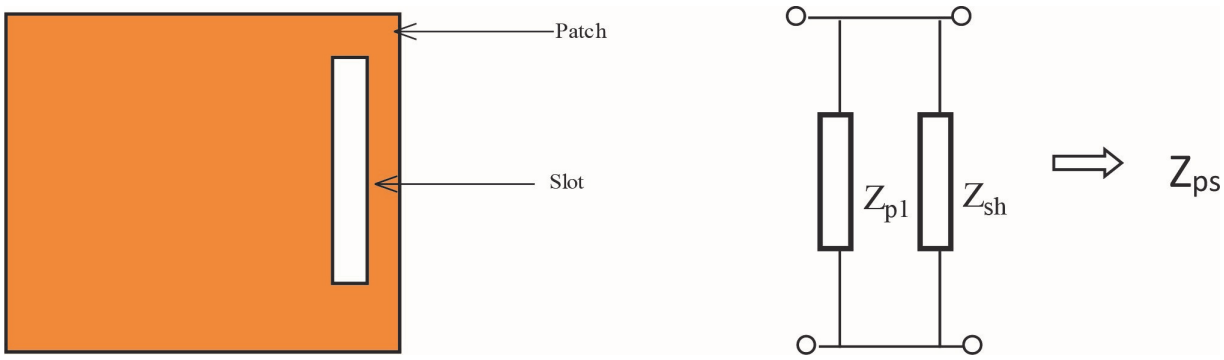

Figure 1.4: Top view of slot loaded MSAs and its equivalent circuit diagram [2]

1.2.2 Feeding techniques of MPA

MPA feeding techniques can be classified into two main categories: direct and indirect contact. Direct contact is where the power is directly inserted to the radiating patch, microstrip line and coaxial line are the most common ones. Whereas, indirect contact is where the power is fed via coupling between the conductor sheet and the microstrip line, aperture coupling and proximity coupling are the well-known among this category.

a) Microstrip Line Feed

a strip directly connected to the patch. the strip impedance may differ from that of the patch, one of the techniques to match both impedances is to add an inset cut to the patch to achieve a succeful feeding.

b) Coaxial Feed

from the general fact that the coaxial cable has inner and outer conductor, the inner is connected to the patch through the dielectric substrate while the outer one is connected to the ground plane. The input impedance can be controlled from changing the position of the feed.

c) Aperture Coupled Feed

This technique adopts a different configuration where the radiation patch is totally separated from the feed line by the ground plane with an aperture to provide the power transmission.

d) Proximity Coupled Feed

like the previous technique, there are also two substrates. The microstrip feed line lies between the two substrates whereas the radiating patch is placed on the upper substrate. Figure 1.5 below shows all the mentioned techniques

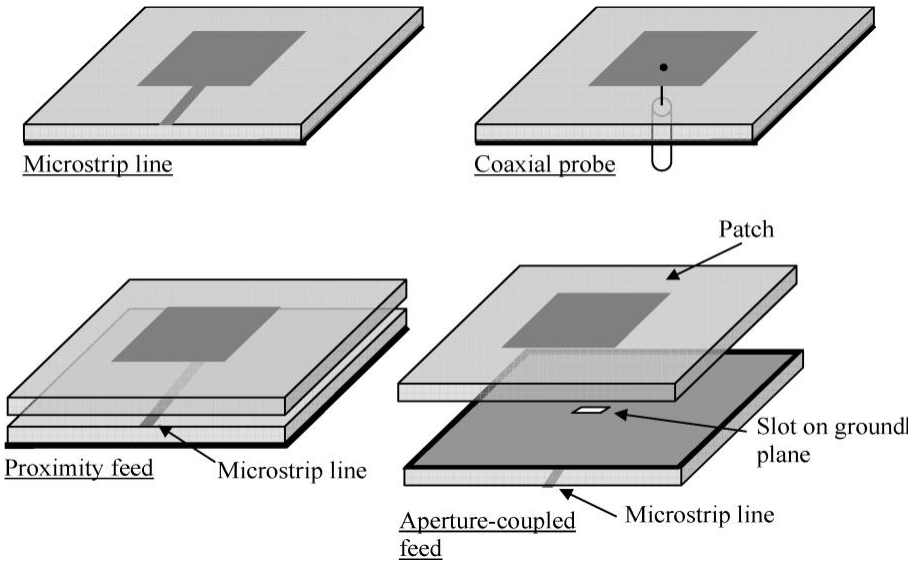

Figure 1.5: Microstrip Patch Antennas feeding techniques [3]

1.2.3 Stacked MSAs

Stacking of MSAs means having two or more dielectric substrate of different or same thickness that is kept over each other or one can say the toppling of one substrate over the other.

1.3 Basic parameters

Before designing any antenna, several antenna characteristics should be taken into consideration. Generally, they are identified by input impedance, return loss, directivity, radiation pattern, and bandwidth. Some of the basic parameters are described:

1.3.1 Input Impedance

Z_{in} is the impedance presented by an antenna at its terminals, or the ratio of the voltage to current at a pair of terminals, or the ratio of the appropriate components of the electric to magnetic fields at a certain point [1]. It's represented as follows:

$$Z_{in} = R_{in} + jX_{in} \tag{1.2}$$

Where R_{in} is the real part of the input impedance, and X_{in} is the imaginary part.

1.3.2 Reflection Coefficient

Testing any antenna requires some essential parameters such as the reflection coefficient, which deals basically with how perfectly the impedance matching between the two ports is done.

$$\Gamma = \frac{Z_{in} - Z_0}{Z_{in} + Z_0} \tag{1.3}$$

Where Z_{in} is the input impedance of the antenna and Z_0 is the characteristic impedance of the transmission (feed) line.
S11 below -10dB means at least 90% input power is delivered to the antenna and the reflected power is less than 10%. This value is sufficient for many applications. The minimum frequency given by the return loss is taken as resonant frequency of the device [7].

1.3.3 Voltage Standing Wave Ratio (VSWR)

VSWR is a numerical value that describes how well the antenna impedance is matched to the feedline impedance. This numerical quantity is always real and positive. VSWR is a function of the reflection coefficient, equation (1.4) defines VSWR [8]:

$$VSWR = \frac{1 - |\Gamma|}{1 + |\Gamma|} \tag{1.4}$$

1.3.4 Directivity

The directivity of an antenna is defined as the ratio of the radiation intensity U in a given direction from the antenna to the radiation intensity averaged over all directions U_0. The average radiation intensity is equal to the total power P_r radiated by antenna divided by 4π. In mathematical form can be written as:

$$D = \frac{U}{U_0} = \frac{4 \times \pi \times U}{P_r} \tag{1.5}$$

If the direction is not indicated, the maximum radiation direction is considered which implies the maximum directivity and equation ‘(1.5) becomes [1]:

$$D_{max} = \frac{4\pi U_{max}}{P_r} \tag{1.6}$$

1.3.5 Gain and Efficiency

The gain is a parameter that is unique for each type of antenna. It is defined as the ratio of the radiation intensity in a certain direction to that resulted from an isotropic antenna radiation of the input power [1]. Also, antenna gain is defined as antenna directivity times a factor representing the radiation efficiency, this efficiency is defined as the ratio of the radiated power (P_r) to the input power (P_i). The input power is transformed into radiated power and surface wave power while a small portion is dissipated due to conductor and dielectric losses of the materials used [9]. In mathematical form can be written as:

$$G = 4\pi \frac{(radiation \quad intensity)}{(total \quad input \quad power)} = \frac{(4\pi U)}{P_{in}} \tag{1.7}$$

$$\eta = \frac{p_{rad}}{P_{in}} \tag{1.8}$$

1.3.6 Bandwidth

Broadly speaking, the bandwidth refers to the useable range of frequencies that includes the antenna’s resonant or working frequency, which centralizes the band. The kind and size of the antenna determines how wide and narrow the BW is. It is usually determined from the graph of S11 by the intersecting the -10 dB level or line with the S11 graph.

1.3.7 Radiation Pattern

Radiation pattern describes the strength of the radiated field distribution as a function of space coordinates. In most cases, it is represented in 3D or 2D in the far-field region and usually in polar format [1].

1.4 Introduction to Multiple Input-Multiple Output Systems

Multiple input, Multiple output (MIMO) systems have been one of the most active areas of research and development in the broad field of the wireless communications. These systems enhance the data transferring rate and reduce the probability of error by taking advantage of multiplexing and diversity, respectively [10]. However, MIMO systems face some challenges such as mutual coupling, which affects the antenna characteristics by reducing the efficiency, increasing the correlation and coupling power and reducing the radiated power [11]. There are many considerable works that have been conducted to deal with such challenges. Among the available solutions is increasing the distance between antennas which is undesirable because this procedure will increase the system's overall size which is not functional for most mobile applications. To solve this problem many technologies have been invented to keep the size within the suitable dimensions. In this section, we will see some generalities about MIMO antenna systems.

1.5 Diversity Techniques

1.5.1 Space Diversity

Two closely coupled antenna radiators can be de-correlated using the space variation. The space variation is the key of this approach to achieve low mutual coupling. all types of MIMO antennas like conventional and non-conventional shaped monopole, dipole etc. use the space diversity. The mutual coupling in this technique is studied in terms of ground and patches, separation and orientation of the radiators [12].

1.5.2 Pattern Diversity

Pattern diversity imposes orthogonality by producing spatially (angularly) disjoint radiation patterns. This is done by shaping the radiation patterns associated with different ports. External beam-forming can be used to generate pattern diversity [13].

1.6 Mutual Coupling Reduction Techniques

As stated before any MIMO antenna system should be constructed in a limited space using a suitable isolation technique to minimize the coupling effect and to have a compacted design for the specific application. Many techniques were developed for this task and some of them were used in this report work. Placing the system radiating elements in an orthogonal orientation can reduce the mutual coupling. Slots are one of the key methods for the decoupling purpose, they can take many shapes depending on the needed applications. In addition, stubs also are widely used for the isolation task; they can have many shapes and positions. Stubs and slots can be combined in same system for better results. Furthermore, the defected ground structure (DGS) is also a wildly adopted technique. This method uses slits placed on the ground plane. It is functional for the reduction of the antenna size and helps suppress the coupling fields between the MIMO elements.

1.7 MIMO Applications

1.7.1 Data Rate Extension

MIMO with low bandwidth and high spectral efficiency solves the problem of high speed and low speed users. In MIMO 1 Gbps data rate is achieved with 20 MHz bandwidth only. MIMO with different modulation like binary phase shift keying (BPSK), quadrature phase shift keying (QPSK), and quadrature amplitude modulation (QAM), offers variable data rates [12].

1.7.2 Power Saving

Unlike other systems like SISO, MIMO does not consume much power. Therefore, it is suitable for wireless applications[12].

1.7.3 Capacity Enhancement

Capacity of MIMO is very high and is not dependent completely on the bandwidth. It increases linearly. The Capacity is affected by the signal to noise ratio (SNR)[12].

1.8 Conclusion

This chapter included an introduction and description of MPAs as well as basic parameters, feeding techniques, and analysis approaches. When examining the antenna performance, characteristics like radiation pattern, gain, and reflection coefficient are very important. Additionally, MIMO antenna systems were showcased. Also addressed where the basic methods for improving MIMO antenna performance, such as isolation.

Chapter 2

Design and Analysis of Fractal Pentagonal Ring Microstrip Patch Antenna

2.1 Introduction

This chapter presents the study and design of a microstrip patch antenna based on a pentagonal fractal ring. Additionally, the suggested design evolution stages are examined. The first step in the design process is to design Antenna 1, a straightforward pentagonal fractal ring patch antenna supplied by a Y-shaped transmission line printed on the front side of the FR-4 substrate with a height of $h = 1.6mm$ and a relative permittivity ϵ_r of 4.3 and a partial rectangular ground plane is printed on the back side of the substrate. Next, in order to obtain Antenna 2, a first-iterative fractal pentagonal ring is introduced. The only change made to Antenna 1 is the substitution of the sides of the pentagonal ring by a square shaped arm. Ultimately, antenna 3 is derived by converting the square branches of the pentagonal ring to a triangular shaped branches in order to center the resonant frequency at 3.5GHz. A full wave simulator CST (computer simulation technology) is used to design the antennas and to simulate the reflection coefficient, current distribution, and radiation patterns .

2.2 Design of Fractal Pentagonal Ring Antenna

2.2.1 Pentagonal Ring Patch Antenna (PRPA)

This design namely Antenna consists of a pentagonal ring radiating element attached to Y-shaped transmission feedline printed on the front side the FR-4 substrate and a simple rectangular ground printed on its back side as shown in Figure 2.1. The pentagon dimension is a side length of $S = 7.1mm$ and a thickness of $t = 0.4mm$. Figure 2.2 shows the corresponding simulated reflection coefficient.

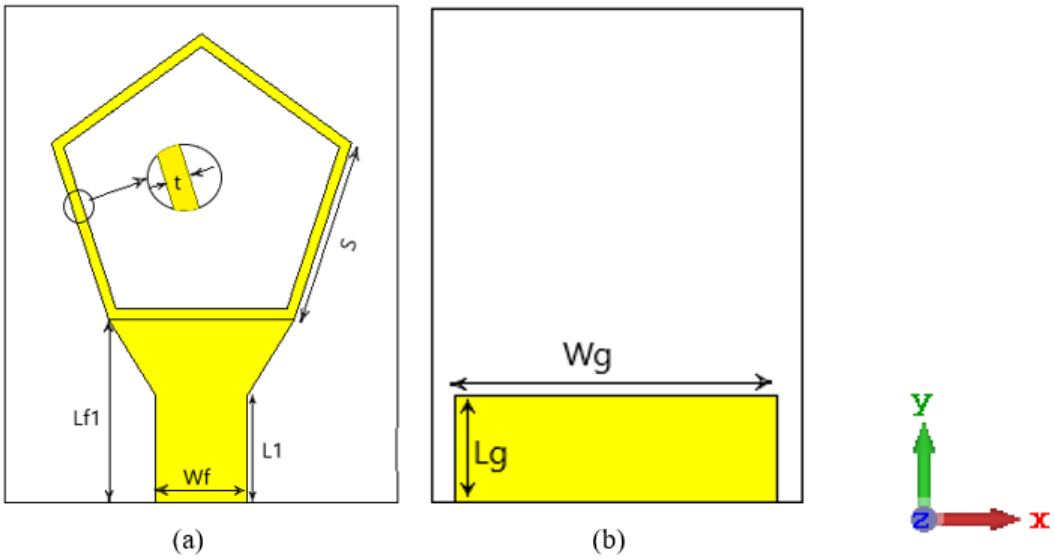

Figure 2.1: Pentagonal ring antenna (a) front view (b) back view for L1=4.1mm, Wf=3.5mm, Lf1=7mm, Wg=13mm and Lg=4.3mm.

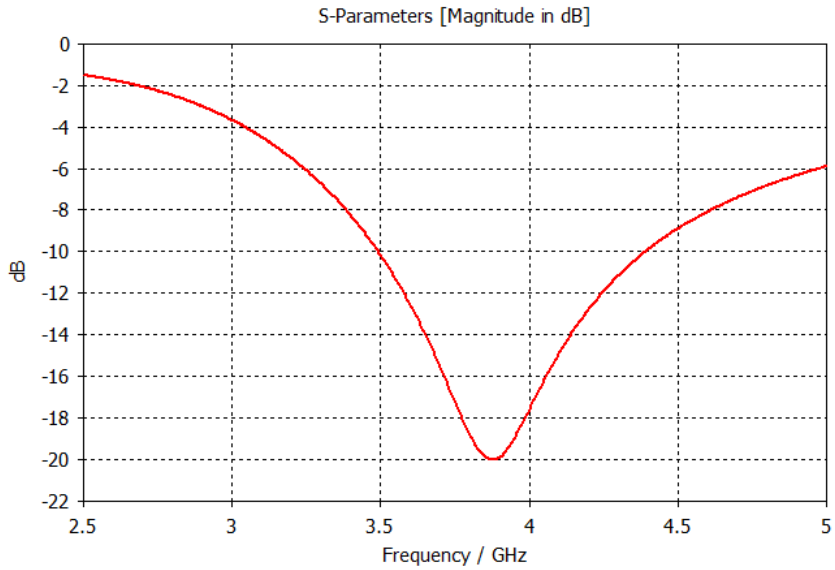

Figure 2.2: Simulated reflection coefficient for PRA

From Figure 2.2, it is clear that this antenna does not cover the 3.5 GHz intended operating frequency. Consequently, an update to the geometry of the antenna has to be done to cover the needed operating frequency.

2.2.2 Fractal Pentagonal Ring Antenna (FPRA)

By substituting the strait sides of the pentagonal rind by rectangular open rings of length D and width S1 the second FPRA is designed as shown in Figure 2.3. It worth to mention that all the geometrical dimensions are kept unchanged as the previous antenna (RRPA). The rectangular shaped strips are added to increase the electrical size of the antenna and reduce the resonant frequency without increasing the antenna dimension. Figure 2.4 illustrates the result of the modification that has been done on the simulated reflection coefficient. It can be seen from the figure that resonant frequency is significantly decreased and the resulted structures covers the 3.5GHz WiMAX band.

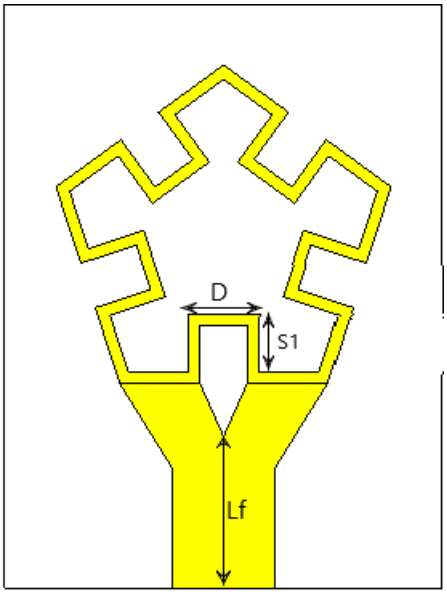

Figure 2.3: Geometry and configuration of the FPRA. for D=2.4mm , S1=2.4mm and Lf=5.2mm.

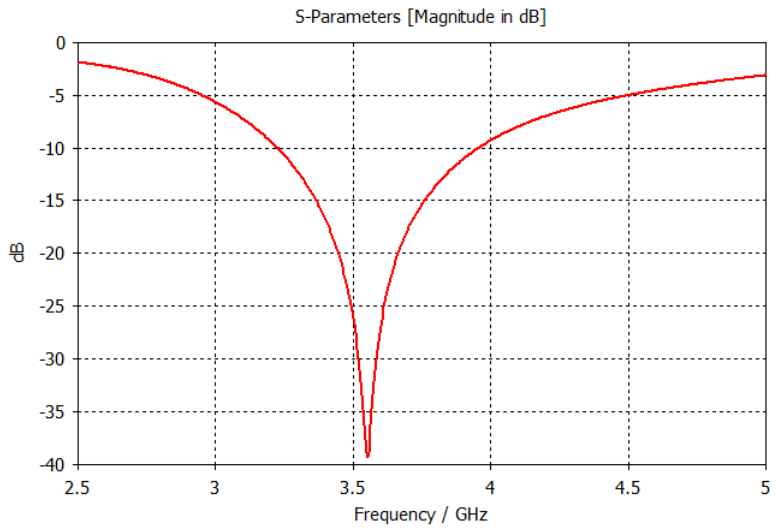

Figure 2.4: Simulated reflection coefficient for FPRA

2.2.3 Modified Fractal Ring Antenna (MFRA)

In the aim of centring the resonant frequency at 3.5GHz without changing the antenna dimensions, the rectangular branches are substituted by trapizoidal ones to derive the MFRA. Figure 2.5 depicts the structure geometry along with its overall dimensions. The gemetrical parameter of the MFRA are given in Table 2.1.

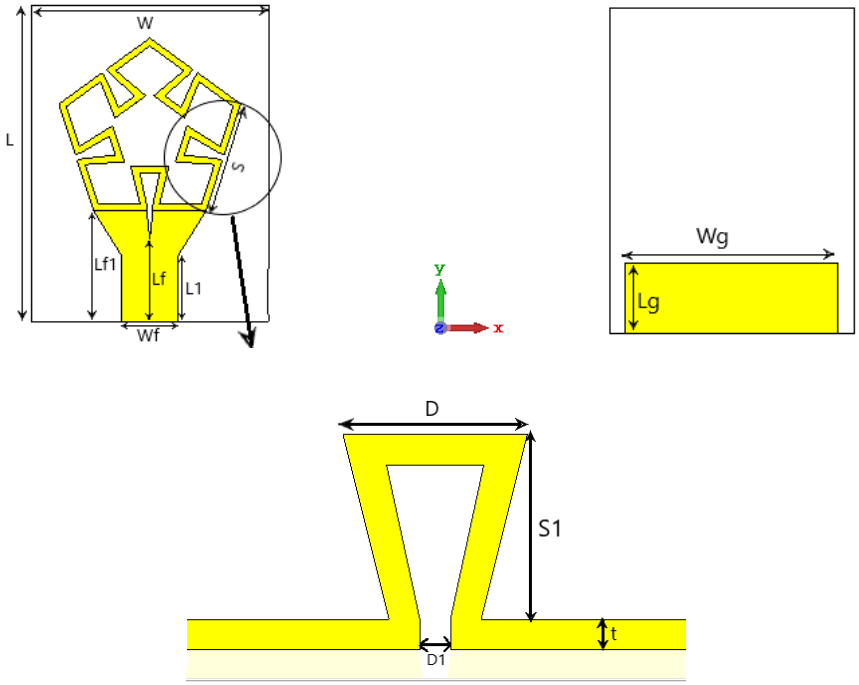

Figure 2.5: Geometry and configuration of the MFRA

Table 2.1: Geometric dimensions of the MFRA

Parameter	W	L	S	S1	D	D1	t	Wf	Lf	Wg	Lg	L1	Lf1
Value(mm)	15	19	7.1	2.4	2.4	0.4	0.4	3.5	5.2	13	4.3	4.1	7

2.3 Parametric Study

A parametric analysis is conducted to examine the impact of critical geometrical factors, which have the greatest influence on antenna performance. One parameter at a time is changed during the simulation, with the remaining parameters kept constant.The investigation of the reflection coefficient response as a function of frequency by altering the pentagon side length is covered in the next section.

2.3.1 Effect of Side Length S on The Reflection Coefficient

Figure 2.4 shows the simulated reflection coefficients for different values of side length (S). It can be seen that by increasing the side length S from 6.5 mm to 8 mm, the operating band shifts toward lower frequencies side. This is expected since the current path on the

fractal ring will be increase with increasing values of S. The considered value of S is 7.1 mm since it is the best matching value.

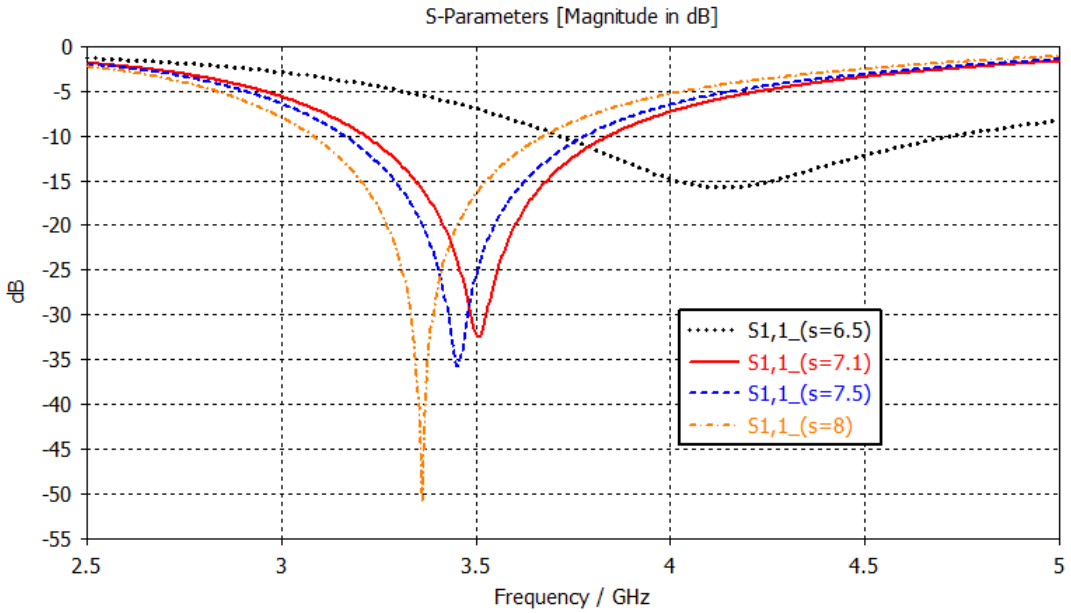

Figure 2.6: Effect of side length variation on the Reflection Coefficient

2.3.2 Effect of S1 on The Reflection Coefficient

From figure 2.7 it can be clearly seen that by varying the length S1 from 1.8mm to 2.6 mm the length is increased and the operating band shifts toward lower frequencies side.

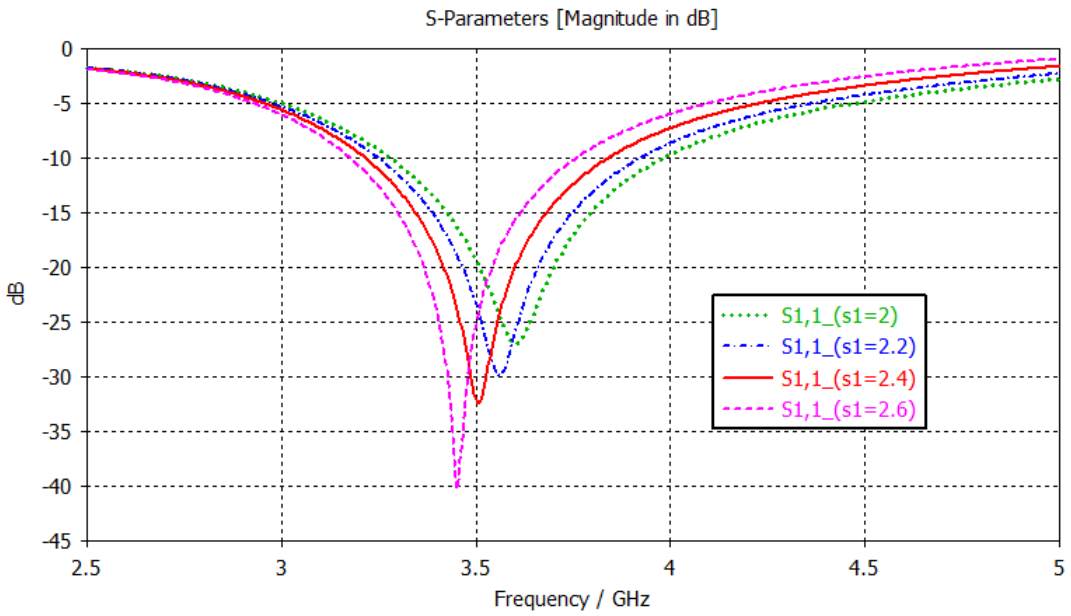

Figure 2.7: Effect of the length S1 variation on the Reflection Coefficient

2.3.3 Effect of the Length D1 on the Reflection Coefficient

Figure 2.8 shows the simulated reflection coefficients as function of D1. It is clearly seen that by increasing the length D1 from 0.4 mm to 2 mm by a step of 0.8 mm, the antenna operating band moves towards lower frequencies with improving impedance matching. It clear that the antenna resonant frequency is centred at 3.5 for D1=0.4mm. The value of D1 can not be further reduced for practical limitations.

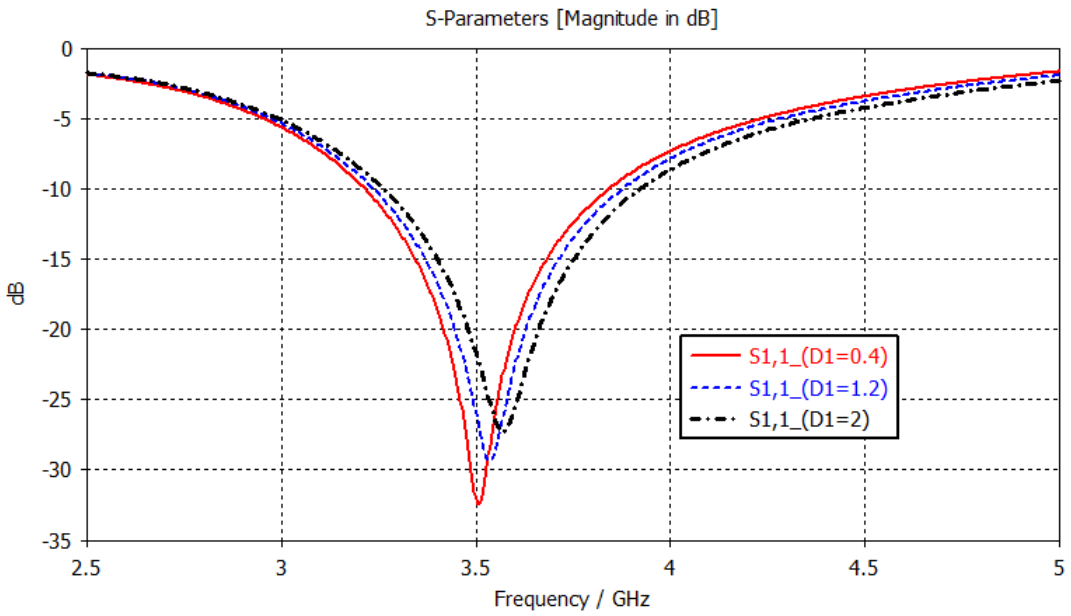

Figure 2.8: Effect of D1 variation on the Reflection Coefficient

2.3.4 Effect of the Feed Line Width Wf on the Reflection Coefficient

Varying the feed line width of an antenna impacts the S11 parameter by affecting impedance matching, resonance frequency and bandwidth. A wider feed line generally has a lower characteristic impedance. If the feed line impedance does not match the antenna impedance, it can result in higher S11 values, indicating more power is reflected and less is radiated. A narrower feed line has a higher characteristic impedance. Figure 2.9 shows the effect of varying the feed line width Wf on S11. At the value of 3.5 mm, it is evident that strong impedance matching and a broader bandwidth are obtained. In contrast, the other values of feed line width did not produce better outcomes in terms of impedance matching and bandwidth.

2.3.5 Effect of Fractal Ring Thickness t on the Reflection Coefficient

The pentagonal ring's width t, can vary from a few millimeters to a few centimeters. Through simulations, It is found that the ideal value which meet the requirement of resonant

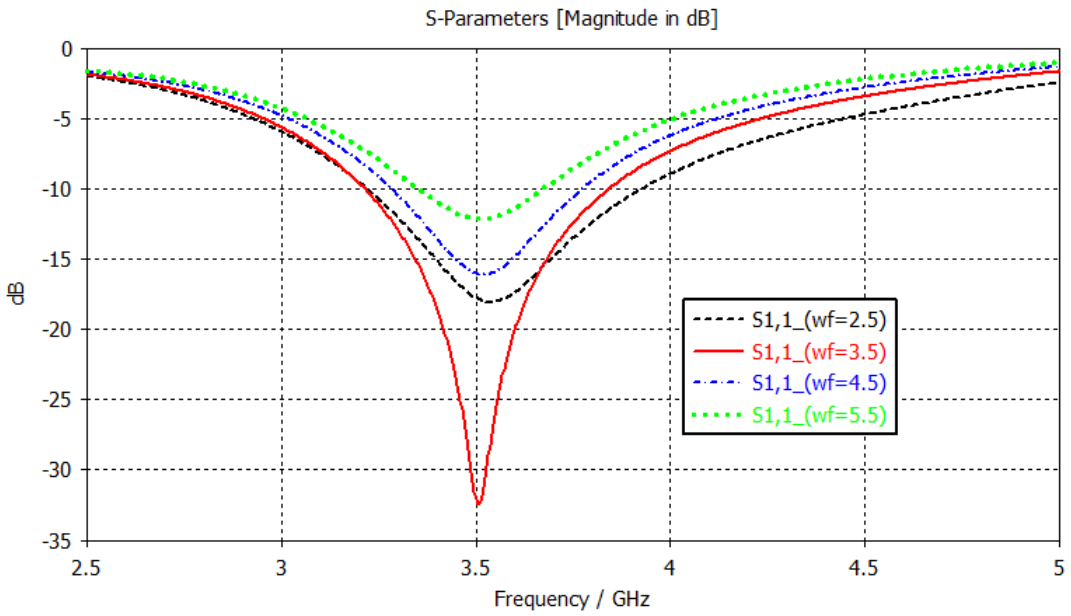

Figure 2.9: Effect Wf on the antenna reflection coefficient

frequency is t=0.4mm as shown in Figure 2.10

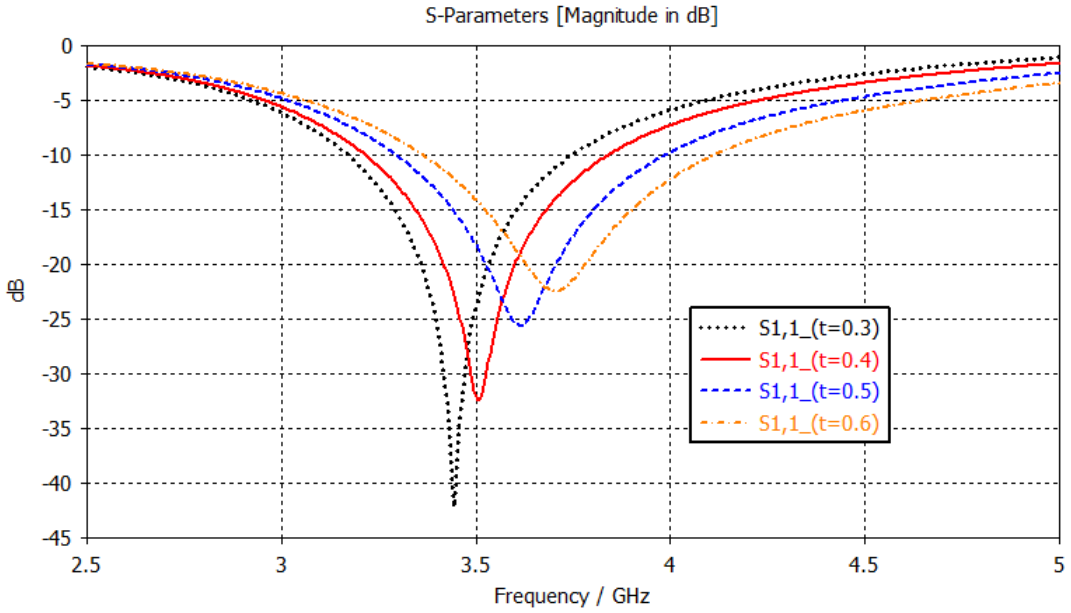

Figure 2.10: Effect of the length t variation on the Reflection Coefficient

It is clearly seen that by increasing the width t from 0.3 mm to 0.6 mm by a step of 0.1 mm, decreasing the antenna dimension, the antenna operating band moves slowly toward higher frequencies. Accordingly, t assure fine tune of the antenna resonant frequency. For

the mentioned reason, it is chosen to be 0.4 mm.

2.3.6 Design Evolution

In this section the three considered structures, shown in Figure 2.11, are compared in terms of reflection coefficient and impedance bandwidths. The three designs have same dimensions of $15 \times 19mm^2$. It can be observed from simulated reflection coefficients shown in Figure 2.12 that Antenna 1 (PRPA) operates in the frequency band extending from 3.5 to 4.4 GHz while Antenna 2 (FPRA) works in the frequency band [3.22GHz -3.95 GHz] and covers widely intended application. The final structure Antenna 3 operates in the frequency band extending from 3.21 GHz to 3.84 GHz centered at 3.5GHz.

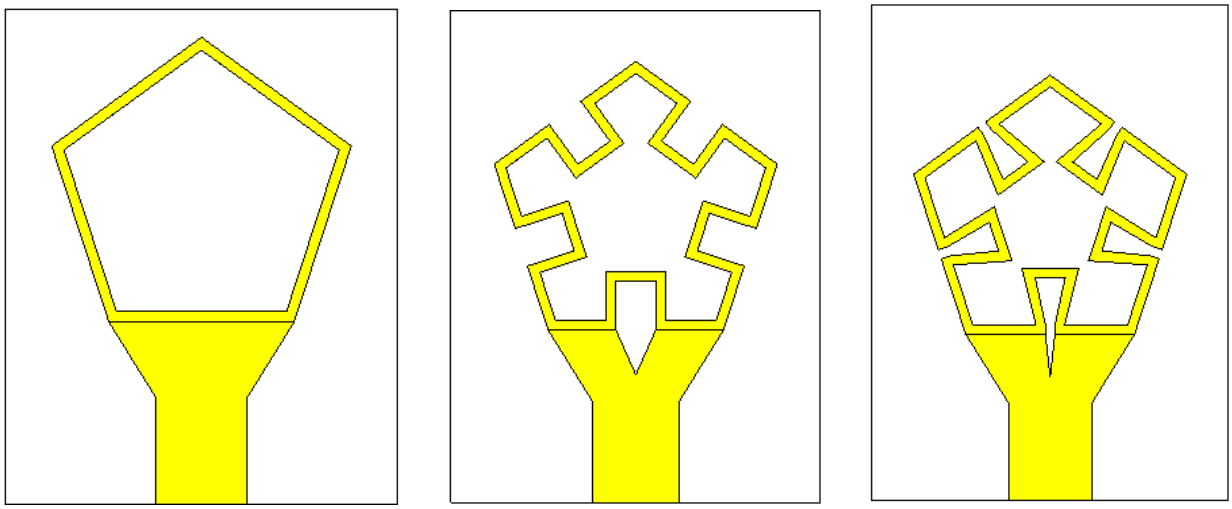

(a) Antenna 1 (b) Antenna 2 (c) Antenna 3

Figure 2.11: Antenna 3 design evolution

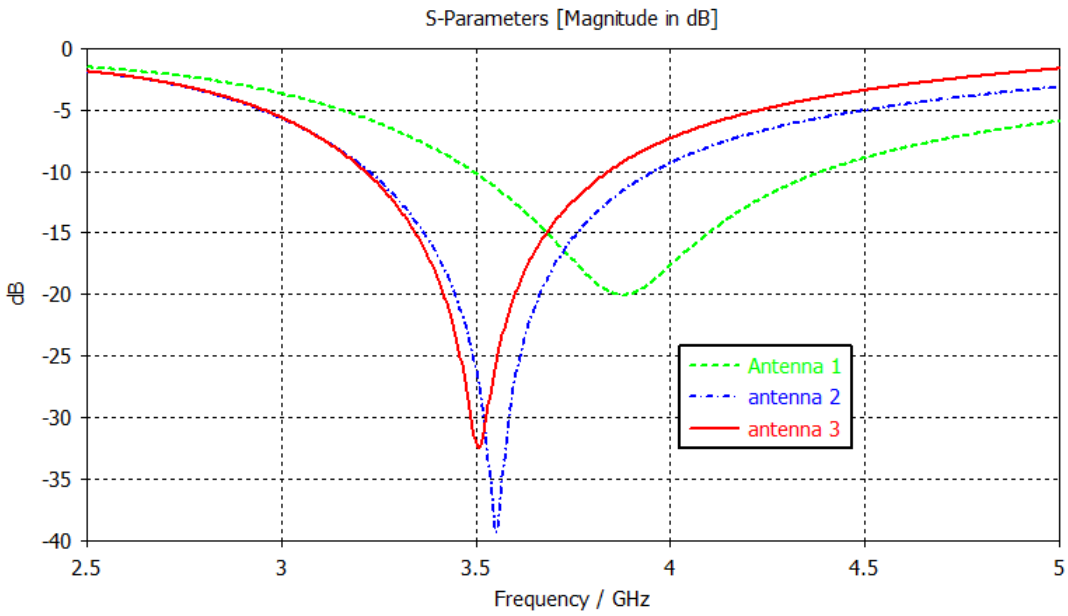

Figure 2.12: Reflection Coefficient versus frequency for different antenna structures

2.4 Current Distribution

Because it illustrates how the current flows through the antenna once it is fed, the distribution of the current throughout the antenna's surface is significant. This data aids in the comprehension of the radiation pattern.

Figure 2.13 shows the simulated current distribution at the resonant frequency 3.5 GHz. It can be clearly seen that the current is mainly concentrated on the two opposite sides of the fractal pentagonal radiating ring as well as the Y-shaped feedline. This confirms the parametric study results which state that any change in the geometrical parameter of the radiating ring will affect the operating frequency band.

2.5 Radiation Pattern

Figure 2.14 shows the simulated 3D radiation pattern of the proposed antenna at 3.5 GHz.It can be seen that the antenna exhibits a radiation pattern that look like a doughnut with maximum gain of 1.15 dBi.

Since the antenna is oriented along the Y-axis, the azimuth angle is ϕ and the

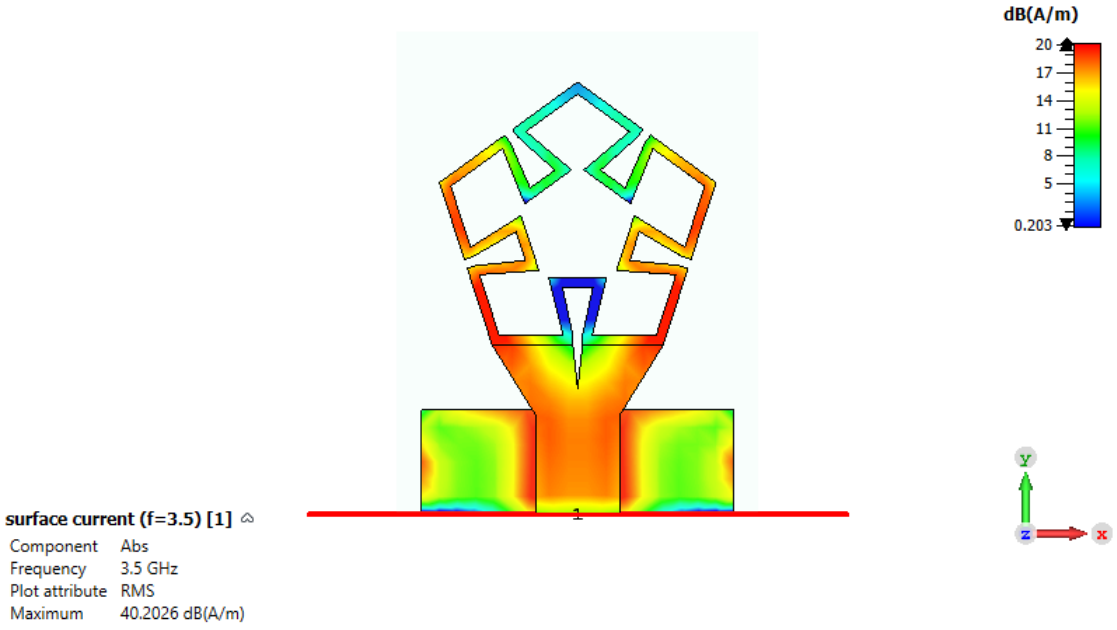

Figure 2.13: Simulated current distribution for Antenna 3 at 3.5 GHz

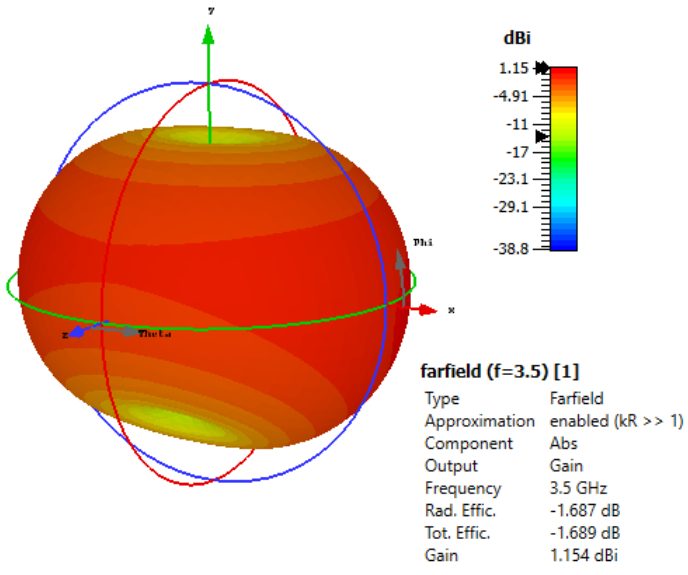

Figure 2.14: The simulated 3D radiation pattern at 3.5 GHz

elevation angle is ϕ. The two-dimensional (y, z) plane (E-plane), is obtained by fixing ϕ to $\frac{\pi}{2}$, and the (x, z) plane(H-plane), is obtained by fixing ϕ to 0. Fig 2.15 and Figure 2.16 respectively shows the E-plane and H-plane radiation patterns at 3.5 GHz. Simulations show that at 3.5 GHz, the resonator produces an omnidirectional pattern in the H-plane, while a figure eight pattern in the E-plane.

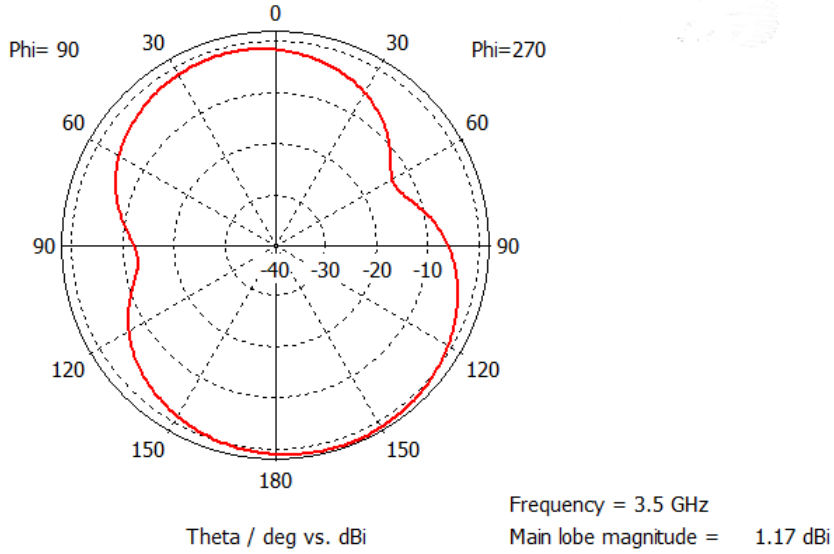

Figure 2.15: The 2D radiation pattern at 3.5 GHz of the E-plane

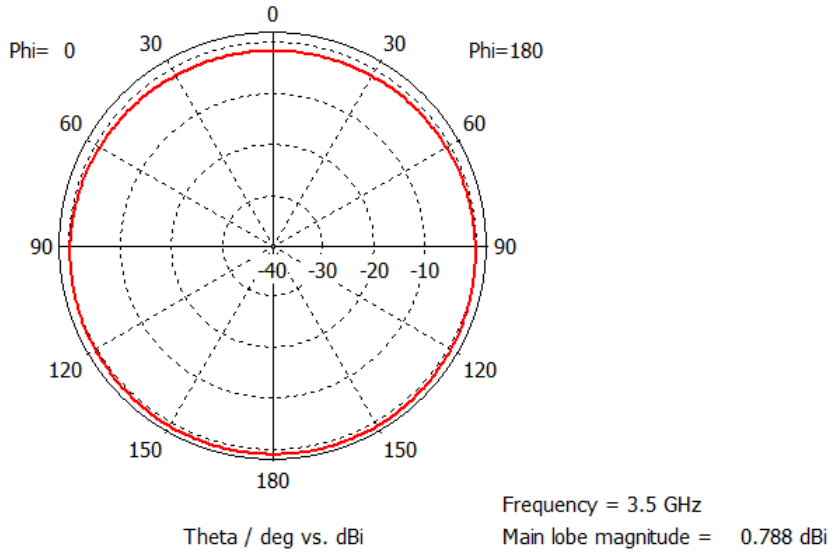

Figure 2.16: The 2D radiation pattern at 3.5 GHz of the H-plane

2.6 Experimental Results

For experimental validation of the proposed antenna, the MFRA antenna was fabricated and tested. Figure 2.17 shows the photograph of the fabricated prototype. The fabricated structure reflection coefficient was measured using a vector network analyzer (VNA) operating in the frequency band from 100 KHz to 20 GHz. The measured and simulated return losses are depicted in Figure 2.18 It is observed that the measured and simulated results are in good agreement. The measured -10dB impedance bandwidth is 530 MHZ(3270-3800 MHz, 15.14%) covering largely the 3.5 GHz WiMAX band.

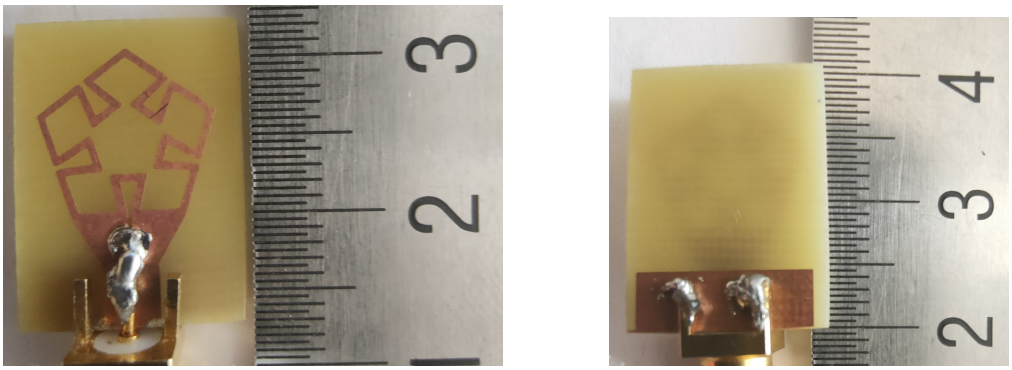

(a) Front view (b) Back view

Figure 2.17: Photograph of the realized antenna

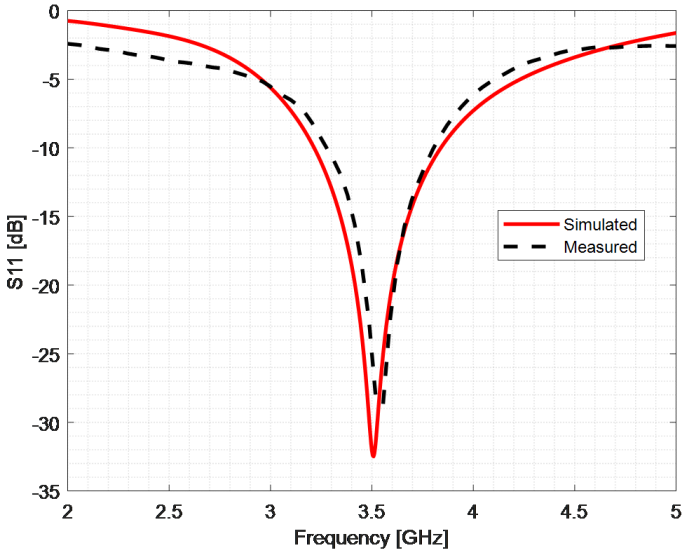

Figure 2.18: he measured and simulated return losse

2.7 Conclusion

In this chapter, a microstrip patch antenna based on a pentagonal fractal ring has been designed, studied and tested. To obtain the ideal design, a stepwise process and parametric studies have been carried out. In the next chapter, the proposed antenna will be used as antenna element in a two port MIMO antenna.

Chapter 3

Design and Analysis of Two-Port MIMO Antenna Based on a Fractal-Ring Radiating Element

3.1 Introduction

The analysis and design of two- port MIMO antenna operating at 3.5GHz will be covered in this chapter. The stages of design evolution that are suggested will also be examined. The antenna element will be the pentagonal-modified fractal ring patch antenna presented in the previous chapter. It will be studied and analyzed in order to assure good isolation between the antenna parts in oreder to have a pattern diversity configuration.
Two identical antennas are positioned orthogonally in polarization diversity configuration. To further enhance the isolation between antenna elements, rectangle-shaped stub is inserted diagonally into the antenna ground plane.

3.1.1 Antenna Structure and configuration

The proposed MIMO antenna is made of two identical pentagonal-fractal ring antenna elements placed orthogonally as depicted in Figure 3.1 This orientation of the antenna element is intentionally chosen for pattern diversity configuration. The top of the antenna elements are separated by a distance De and printed on FR-4 substrate with overall dimensions of Ws x Ls. To achieve higher isolation without increasing the antenna dimensions a rectangular-shaped stub is printed on the back side of the substrate and positioned diagonally across it. The geometrical parameters the proposed MIMO antenna are listed in Table 3.1.

Table 3.1: Geometric dimensions of the proposed MIMO antenna

Parameter	Ws	Ls	S	S1	D	D1	t	Wf
Value(mm)	31.35	31.35	6.4	2.2	2.2	0.4	0.4	3.5
Parameter	Lf	Wg	Lg	L1	Lf1	De	SL	Sw
Value(mm)	5.2	13	4.3	4.1	7	11.31	41	2

3.1.2 Design Evolution

The initial structure namely Antenna 1 is presented in Figure 3.2. Antenna 1 is simply the proposed antenna, described the previous section, without stub. The simulated S_{11} and S_{21}, for Antenna 1 , are shown in figure 3.3 and figure 3.4 respectively. It is noted that Antenna 1 operates in the frequency band [3.35 GHz-4.18 GHz] with an isolation less than

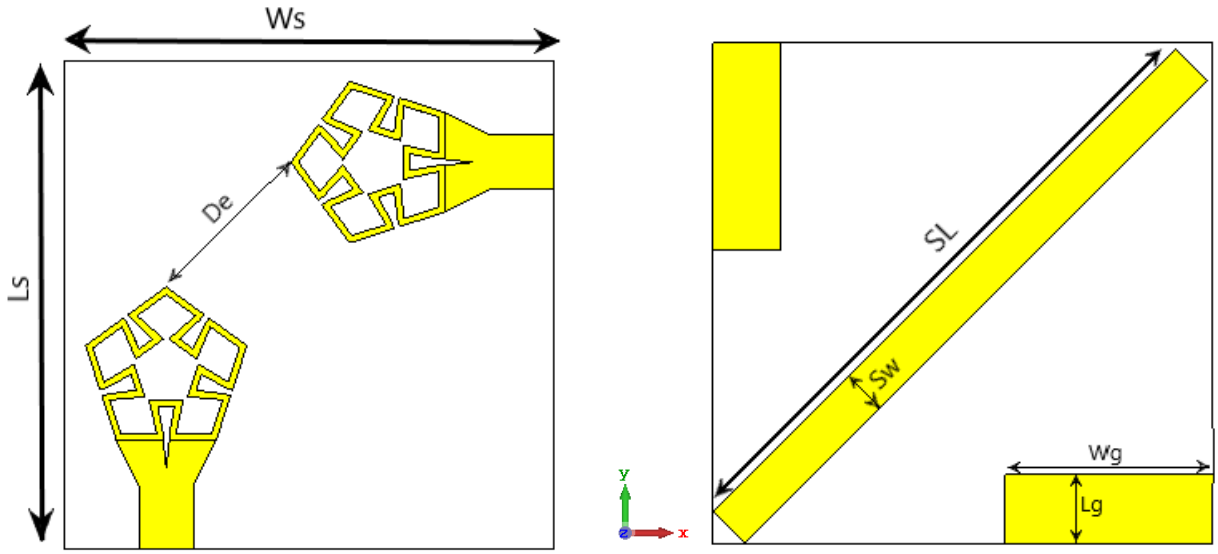

(a) (b) (c)

Figure 3.1: The geometrical configuration of the proposed two-port MIMO Antenna with (a)Front view (b)axis (c)Back view

-12dB. Whereas, the final structure namely Antenna2 with stub width of Sw of 2mm and stub length of 41 mm operates in the frequency band [3.14 dB-3.87 dB] with an isolation less than -19 dB throughout the entire operating band. It is noticed that the reflection coefficient is drastically improved especially at the resonance frequency of 3.5 GHz with a level of -25dB. Moreover, better isolation is obtained with S_{21} less than -19dB over a frequency band extending from 3.15 GHz to 3.86 GHz.

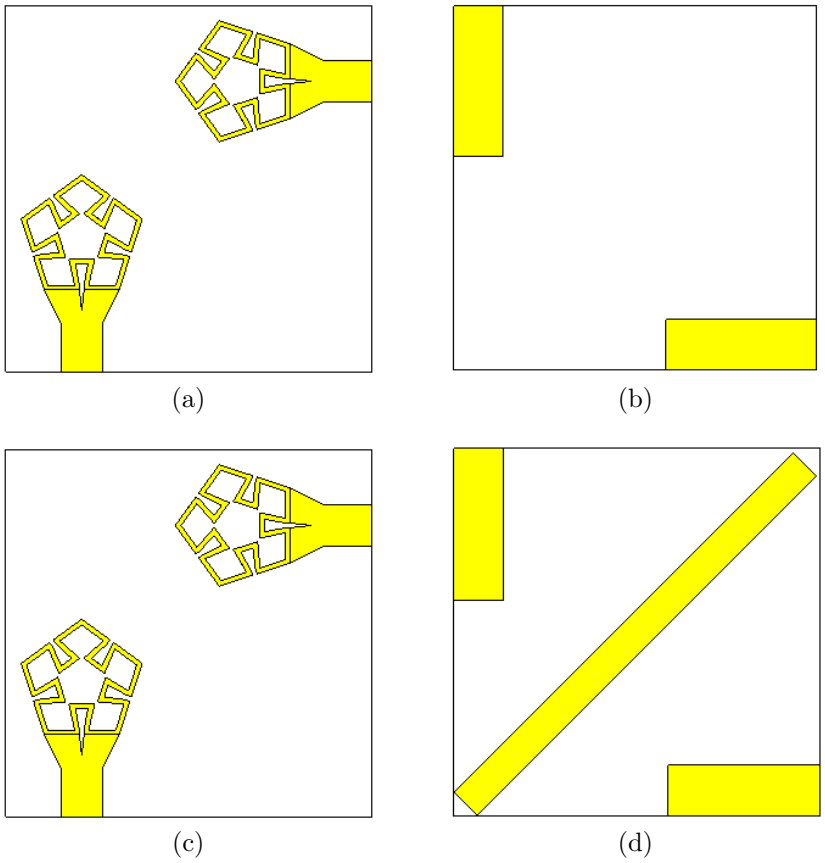

Figure 3.2: Design evolution: Antenna 1 (a)Front view and (b) Back view. Antenna 2: (c)Front view and (d) Back view.

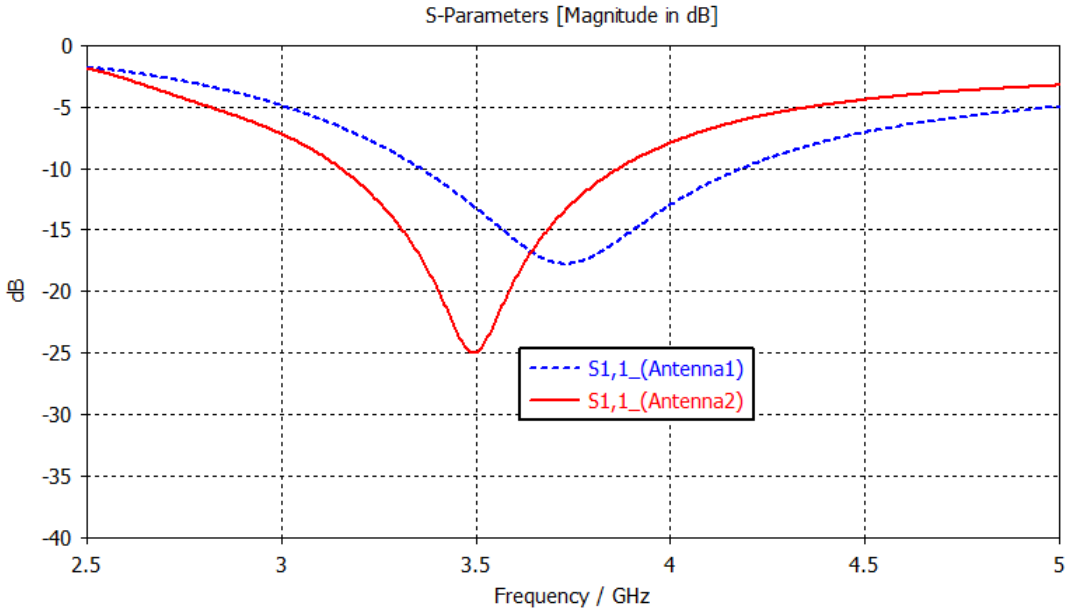

Figure 3.3: Simulated return loss for various antennas involved in the design evolution

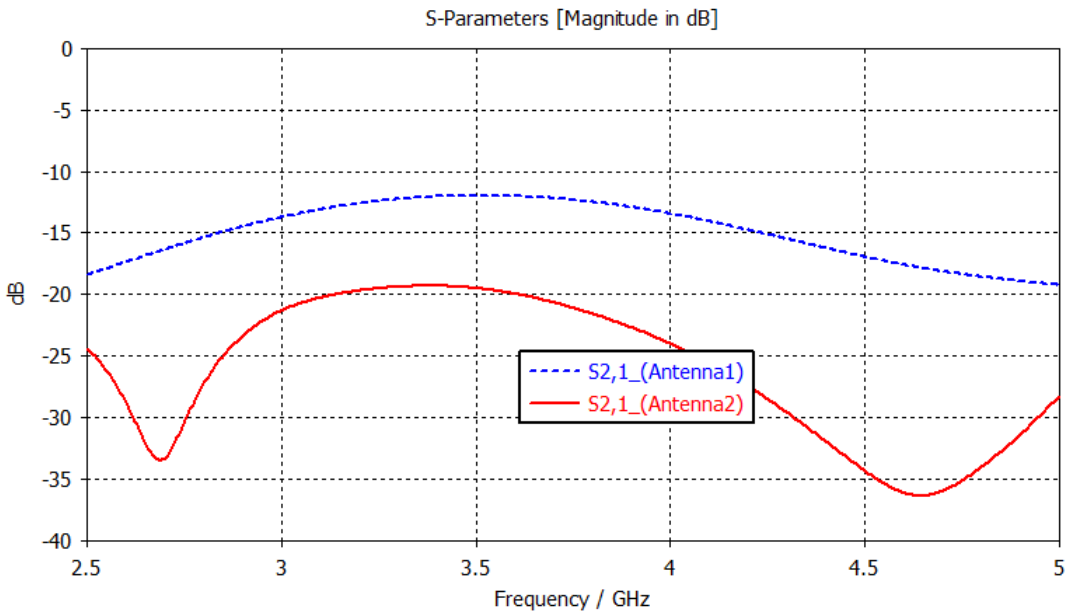

Figure 3.4: Simulated isolation for various antennas involved in the design evolution

3.1.3 Parametric Study

A parametric research is conducted to comprehend the proposed structure's isolation mechanism. One parameter at a time is changing during the simulations, with the kept parameters remaining constant. This part's primary objective is to design the MIMO antenna for the ideal value of S_{21} in order to prevent antenna coupling.

Effect of The Distance De on S_{21}

The simulated S_{21} for various values of De is displayed in Figure 3.5. The considered values of De are of 7, 8.5, 9.9, and 11.3 mm, it is evident that the length De has a slight impact on the isolation. Over the frequency range of 2.5–5 GHz, the isolation is less than -19dB for De=11.31 mm. De is therefore taken to have a value of 11.31mm.

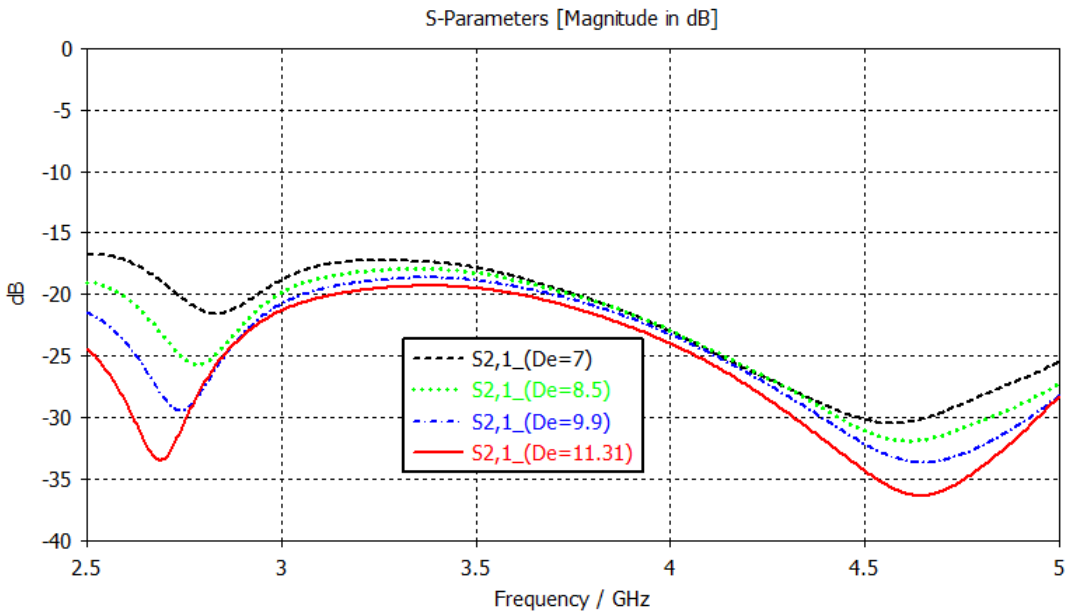

Figure 3.5: Effect of De variation on S_{21}

Effect of The Stub Width Ws on S_{21}

The simulated S_{21} for different values of the stub width Ws is shown in Figure 3.6.The Figure makes it clear that Ws has an impact on isolation. Furthermore, when Ws=2 mm, it is observed that the isolation is less than -19dB for the frequency band spanning from 2.5 to 5 GHz.

Effect of The Stub Length (SL) on S_{21}

The simulated S_{21} for different values of the stub length SL is shown in Figure 3.7.It is clear from the figure that by increasing SL from 15mm to 41mm the S21 level decreases from -12 dB to -19dB.

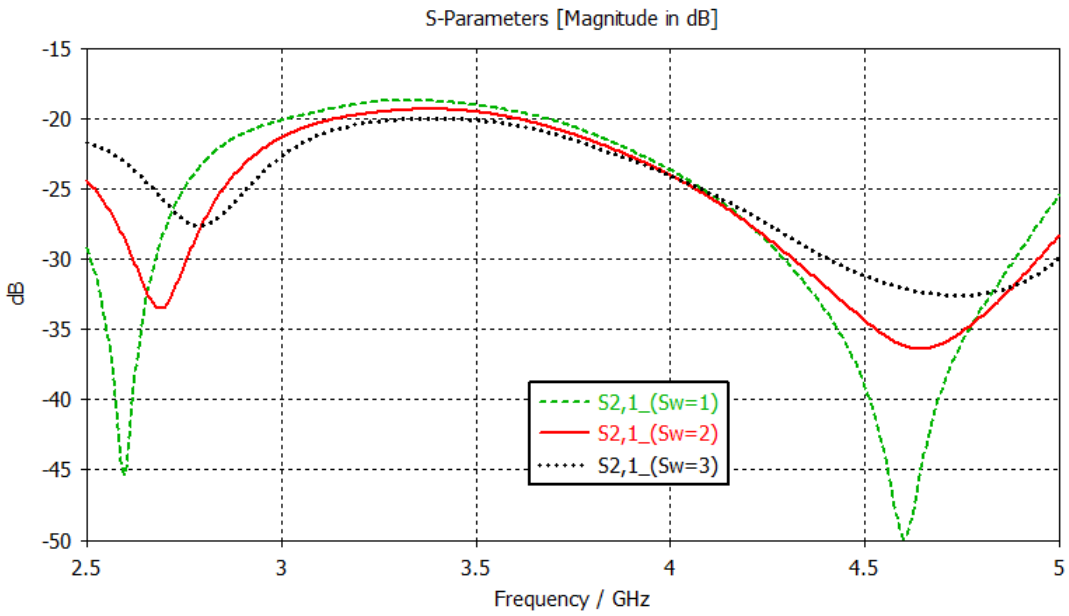

Figure 3.6: Effect of the stub width Ws variation on S_{21}

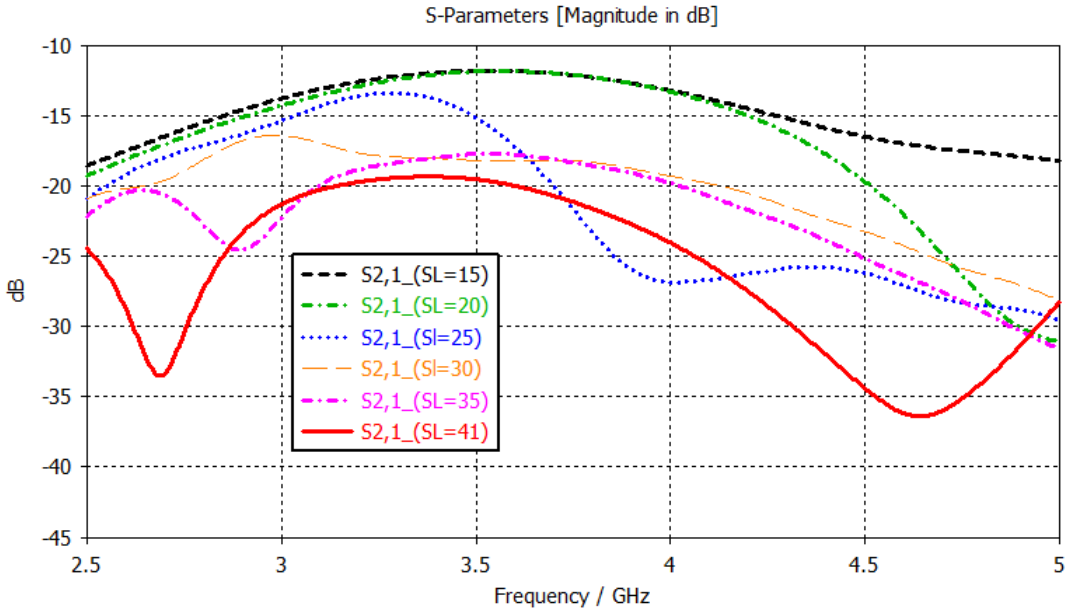

Figure 3.7: Effect of the stub length SL variation on S_{21}

3.1.4 Current Distribution

Figure 3.8 displays the computed current distribution front and back view for the suggested MIMO antenna at the 3.5 GHz resonant frequency. It is evident that when one

abtenna element (the vertical on) is operating, the current is very weak in the center and upper regions of the farctal-ring and is mostly concentrated on the opposite sides of the fractal-ring and on the feedline. There is no current flow for antenna two (horizontal), indicating good isolation between the two elements. Furthermore, the current is largely concentrated on the rectangular-shaped stub. As a result, the ground stub offsets the current flowing from port 1 to port 2, reducing mutual coupling between antenna elements.

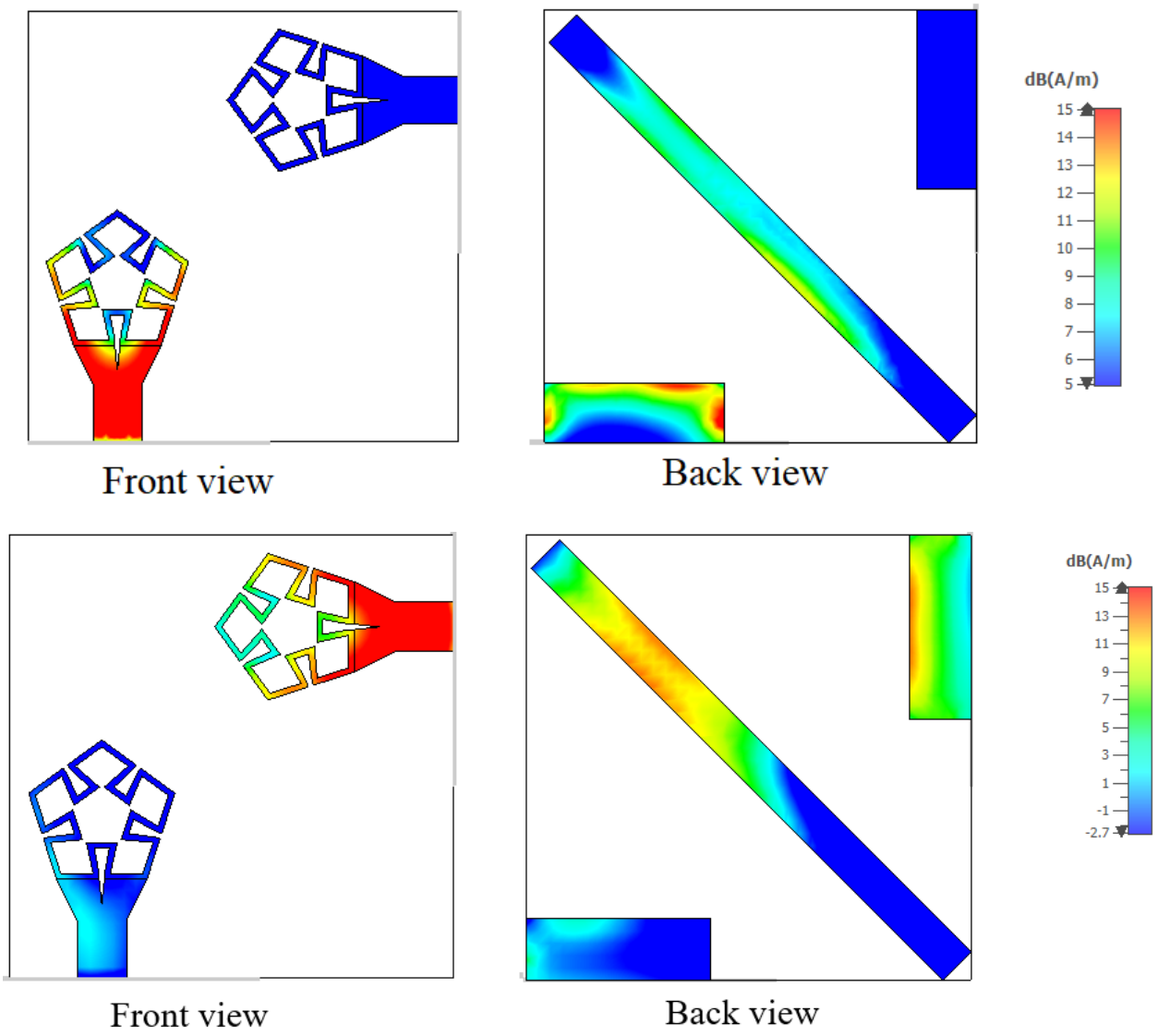

Figure 3.8: Simulated current distribution at 3.5 GHz

3.1.5 Radiation Pattern

Figure 3.9 shows the simulated 3D radiation pattern at 3.5 GHZ. Figures 3.10 and 3.11 show the radiation patterns for the E- and H-planes, respectively. The far-field radiation patterns reveal that the radiation pattern in the H-plane (Figure 3.11) is omnidirectional, whereas in the E-plane (Figure 3.10), it is a dipole-like pattern with peak gain of 1.76 dbi.

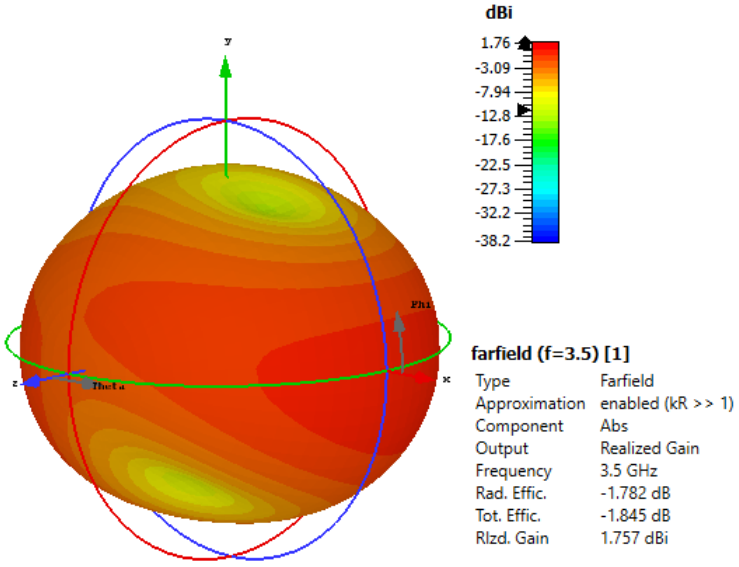

Figure 3.9: The 3D Simulated radiation pattern at 3.5 GHz

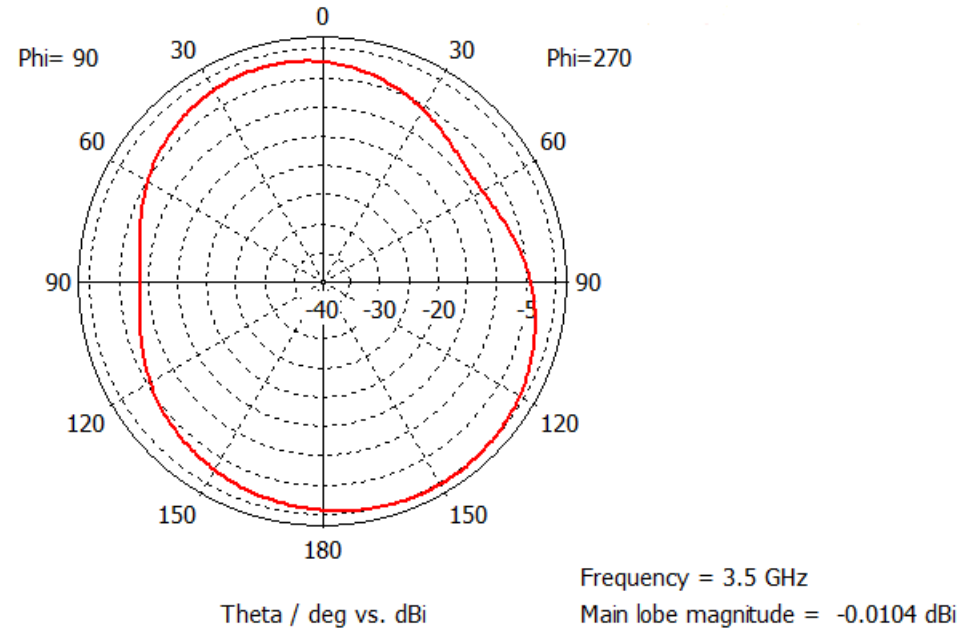

Figure 3.10: Simulated radiation pattern at 3.5 GHz in the E-plane

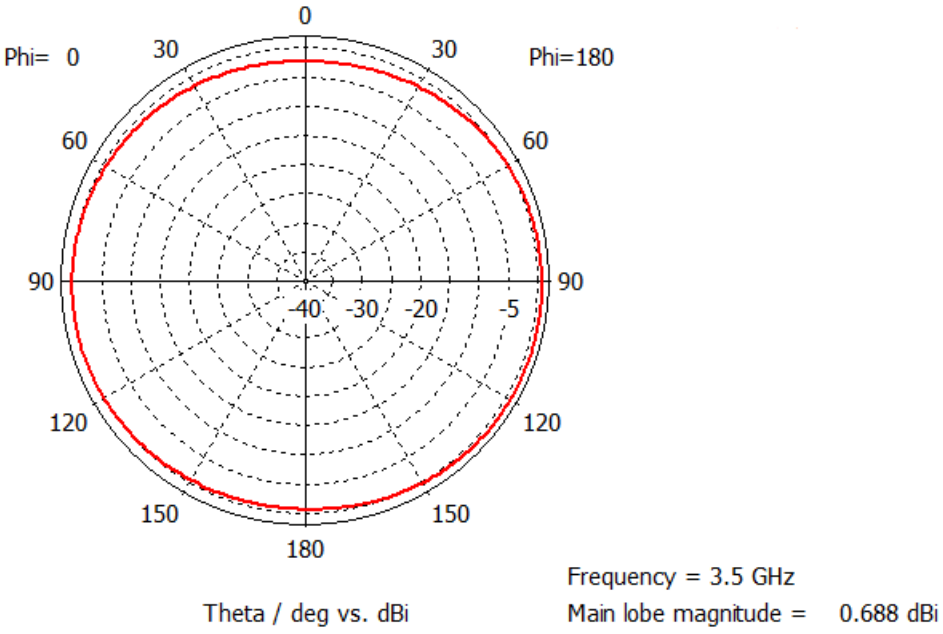

Figure 3.11: Simulated radiation pattern at 3.5 GHz in the EHplane

3.2 Conclusion

The design and analysis of a MIMO antenna with a polarization diversity configuration is presented in this chapter. The 3.5GHz WiMAX application has been covered by the design of the fractal-ring antenna element. The antenna ground plane of the suggested pattern diversity configuration has a rectanglular-shaped stub loaded for better isolation. The resulting structure has a simulated peak gain of 1.76dBi and compact dimensions of 31.35 x 31.35 mm2. It also exhibits an omnidirectional radiation pattern.

General Conclusion

In this work the design of two-element polarization diversity configuration of pentagonal fractal ring monopole antenna has been proposed. The antenna element has been designed to operate in the 3.5 GHz frequency band allotted to the WiMAX application.

Firstly, the antenna element has been designed to operate in the frequency band covering the intended application. An evolution study to produce the final element geometry has been caried out with help of a full wave-based simulator CST. The final structure has a fractal shaped pentagonal ring patch. The proposed structure operates at the frequency band extending from 3.21 GHz to 3.84 GHz and has an omnidirectional radiation pattern which makes it well suited to be used in wireless applications.

Then, two elements have been used to develop a two-port MIMO antenna. The proposed structure consists of two elements placed orthogonally in polarization diversity configuration. The high isolation has been achieved by the insertion a rectangular- shaped stub and by the antenna elements orientation (polarization diversity). The resulted structure has compact dimensions of 31.35x 31.35mm2 and exhibits an omnidirectional radiation pattern with a simulated peak gain of 1.76 dBi.

The proposed fractal ring antenna element has been prototyped and tested and a good agreement has been observed between the simulated and measured results

Bibliography

[1] C. A. Balanis, *Antenna Theory: Analysis and Design.* John Wiley & Sons, Inc., third ed., 2005.

[2] A. Singh, K. Shet, D. Prasad, A. Pandey, and M. Aneesh, *A Review: Circuit Theory of Microstrip Antennas for Dual-, Multi-, and Ultra-Widebands.* 03 2020.

[3] W. Whittow, "Microstrip patch antennas with 3-dimensional substrates," pp. 1–5, 11 2012.

[4] S. Satya and S. Srikant, "An overview on monolithic microwave integrated circuits," *Turkish Journal of Engineering, Science and Technology*, vol. 03, pp. 123–126, 01 2014.

[5] J. Bernhard, P. Mayes, D. Schaubert, and R. Mailloux, "A commemoration of deschamps and sichak's microstrip microwave antennas: 50 years of development divergence and new directions," p. 42, 09 2003.

[6] A. Derneryd and I. Karlsson, "Broadband microstrip antenna element and array," *Antennas and Propagation, IEEE Transactions on*, vol. 29, pp. 140 – 141, 02 1981.

[7] T. Bird, "Definition and misuse of return loss [report of the transactions editor-in-chief]," *Antennas and Propagation Magazine, IEEE*, vol. 51, pp. 166 – 167, 05 2009.

[8] A. Andreev, E. Farr, and E. Schamiloglu, "A simplified theory of microwave pulse compression," 01 2008.

[9] V. Keerthi, "Design of c-band microstrip patch antenna for radar applications using ie3d," *IOSR Journal of Electronics and Communication Engineering*, vol. 5, pp. 49–58, 01 2013.

[10] E. Biglieri, R. Calderbank, A. Constantinides, A. Goldsmith, A. Paulraj, and H. Poor, *MIMO Wireless Communications*. Cambridge University Press, 2007.

[11] M. Jankiraman, *Space-time Codes and MIMO Systems*. Artech House universal personal communications series, Artech House, 2004.

[12] M. Kartikeyan, L. Malviya, and R. K. Panigrahi, *MIMO Antennas for Wireless Communication: Theory and Design*. 2021.

[13] F. De Flaviis, L. Jofre, J. Romeu, and A. Grau Besoli, *Multiantenna Systems for MIMO Communications*, vol. 3. 01 2008.